Designation: C 1683 – 08

Standard Practice for Size Scaling of Tensile Strengths Using Weibull Statistics for Advanced Ceramics[1]

This standard is issued under the fixed designation C 1683; the number immediately following the designation indicates the year of original adoption or, in the case of revision, the year of last revision. A number in parentheses indicates the year of last reapproval. A superscript epsilon (ε) indicates an editorial change since the last revision or reapproval.

1. Scope

1.1 This standard practice provides methodology to convert fracture strength parameters (primarily the mean strength and the Weibull characteristic strength) estimated from data obtained with one test geometry to strength parameters representing other test geometries. This practice addresses uniaxial strength data as well as some biaxial strength data. It may also be used for more complex geometries proved that the effective areas and effective volumes can be estimated. It is for the evaluation of Weibull probability distribution parameters for advanced ceramics that fail in a brittle fashion. Fig. 1 shows the typical variation of strength with size. The larger the specimen or component, the weaker it is likely to be.

1.2 As noted in Practice C 1239, the failure strength of advanced ceramics is treated as a continuous random variable. A number of functions may be used to characterize the strength distribution of brittle ceramics, but the Weibull distribution is the most appropriate especially since it permits strength scaling for the size of specimens or component. Typically, a number of test specimens with well-defined geometry are broken under well-defined loading conditions. The force at which each test specimen fails is recorded and fracture strength calculated. The strength values are used to obtain Weibull parameter estimates associated with the underlying population distribution.

1.3 This standard is restricted to the assumption that the distribution underlying the failure strengths is the two-parameter Weibull distribution with size scaling. The practice also assumes that the flaw population is stable with time and that no slow crack growth occurs.

1.4 This practice includes the following topics:

1.5 The values stated in SI units are to be regarded as the standard per IEEE/ASTM SI 10.

1.6 *This standard does not purport to address all of the safety concerns, if any, associated with its use. It is the responsibility of the user of this standard to establish appropriate safety and health practices and determine the applicability of regulatory limitations prior to use.*

2. Referenced Documents

2.1 *ASTM Standards:* [2]

C 1145 Terminology of Advanced Ceramics

C 1161 Test Method for Flexural Strength of Advanced Ceramics at Ambient Temperature

C 1211 Test Method for Flexural Strength of Advanced Ceramics at Elevated Temperatures

C 1239 Practice for Reporting Uniaxial Strength Data and Estimating Weibull Distribution Parameters for Advanced Ceramics

C 1273 Test Method for Tensile Strength of Monolithic Advanced Ceramics at Ambient Temperatures

C 1322 Practice for Fractography and Characterization of Fracture Origins in Advanced Ceramics

C 1323 Test Method for Ultimate Strength of Advanced Ceramics with Diametrally Compressed C-Ring Specimens at Ambient Temperature

[1] This practice is under the jurisdiction of ASTM Committee C28 on Advanced Ceramics and is the direct responsibility of Subcommittee C28.01 on Mechanical Properties and Performance.

Current edition approved Jan. 1, 2008. Published January 2008.

[2] For referenced ASTM standards, visit the ASTM website, www.astm.org, or contact ASTM Customer Service at service@astm.org. For *Annual Book of ASTM Standards* volume information, refer to the standard's Document Summary page on the ASTM website.

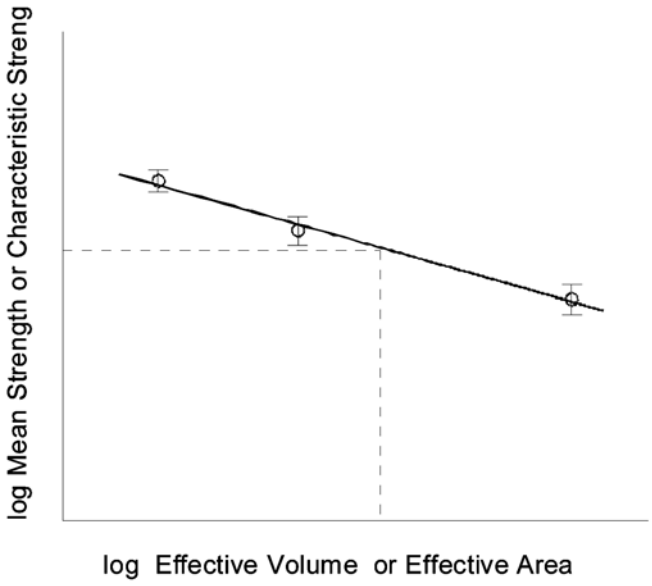

FIG. 1 Strength Scales with Size

C 1366 Test Method for Tensile Strength of Monolithic Advanced Ceramics at Elevated Temperatures
C 1499 Test Method for Monotonic Equibiaxial Flexural Strength of Advanced Ceramics at Ambient Temperature
E 6 Terminology Relating to Methods of Mechanical Testing
E 456 Terminology Relating to Quality and Statistics

3. Terminology

3.1 Unless otherwise noted, the Weibull parameter estimation terms and equations found in Practice C 1239 shall be used.

3.2 For definitions of other statistical terms, terms related to mechanical testing, and terms related to advanced ceramics used in this guide, refer to Terminologies E 6, E 456, and C 1145, or to appropriate textbooks on statistics (**1-4**).[3]

3.3 *Nomenclature*:

A_T = gage area of a uniaxial tensile test specimen
A_{B4} = gage area of a four-point flexure test specimen
A_{B3} = gage area of a three-point flexure test specimen
A_{POR} = gage area of a pressure-on-ring test specimen
A_{ROR} = gage area of a ring-on-ring test specimen
A_{CR} = gage area of a C-ring test specimen
b = thickness of a C-ring
b = width of a flexure test specimen
d = thickness of a flexure test specimen
D = diameter of a round flexure test specimen
D = overall diameter of a ring-on-ring disk test specimen
D_L = loading (inner) ring diameter, ring-on-ring disk specimen
D_S = support ring diameter, ring-on-ring or pressure-on-ring disk specimen
h = thickness of pressure-on-ring or ring-on-ring disk test specimen
k = load factor
L_{gs} = length of the gage section in a uniaxial tensile test specimen
L_{i4} = length of the inner span for a four-point flexure test specimen
L_{o4} = length of the outer span for a four-point flexure test specimen
L_{o3} = length of the outer span for a three-point flexure test specimen
m = Weibull modulus
P_f = probability of failure
r_i = inner radius of a C-ring
r_o = outer radius of a C-ring
t = thickness of a C-ring
R_s = radius of the support ring for pressure-on-ring
R_d = radius of the pressure-on-ring disk specimen
S_E = effective surface area of a test specimen
V_E = effective volume of a test specimen
V_{POR} = gage volume of a pressure-on-ring test specimen
V_{ROR} = gage volume of a ring-on-ring disk test specimen
V_T = gage volume of tensile test specimen
V_{B4} = gage volume of a four-point flexure test specimen
V_{B3} = gage volume of a three-point flexure test specimen
V_{CR} = gage volume of a C-ring test specimen
σ = uniaxial tensile stress
σ_{max} = maximum tensile stress in a test specimen at fracture
σ_1, σ_2, σ_3 = principal stresses (tensile) at the integration points in any finite element
σ_0 = Weibull material scale parameter (strength relative to unit size)
σ_θ = Weibull characteristic strength
$\sigma_{\theta T}$ = Weibull characteristic strength of a uniaxial tensile test specimen

[3] The boldface numbers in parentheses refer to the list of references at the end of this standard.

$\sigma_{\theta B4}$ = Weibull characteristic strength for a four-point flexure test specimen

$\sigma_{\theta B3}$ = Weibull characteristic strength for a three-point flexure test specimen

$\sigma_{\theta CR}$ = Weibull characteristic strength for a C-ring test specimen

$\sigma_{\theta POR}$ = Weibull characteristic strength for a pressure-on-ring test specimen

$\sigma_{\theta ROR}$ = Weibull characteristic strength for a ring-on-ring test specimen

σ^* = an arbitrary, assumed estimate of the Weibull material scale factor

$\bar{\sigma}$ = mean strength

$\bar{\sigma}_T$ = mean strength for a uniaxial tensile test specimen

$\bar{\sigma}_{B4}$ = mean strength for a four-point flexure test specimen

$\bar{\sigma}_{B3}$ = mean strength for a three-point flexure test specimen

$\bar{\sigma}_{CR}$ = mean strength for a C-ring test specimen

$\bar{\sigma}_{POR}$ = mean strength for a pressure-on-ring test specimen

$\bar{\sigma}_{ROR}$ = mean strength for a ring-on-ring test specimen

θ = angle in a C-ring test specimen

4. Summary of Practice

4.1 The observed strength values of advanced ceramics are dependent on test specimen size, geometry and stress state. This standard practice enables the user to convert tensile strength parameters obtained from one test geometry to that of another, on the basis of assumptions listed in 5.5. Using the existing fracture strength data, estimates of the Weibull characteristic strength σ_θ, and the Weibull modulus m, are calculated in accordance with related Practice C 1239 for the original test geometry. This practice uses the test specimen and loading sizes and geometries, and σ_θ and m to calculate the Weibull material scale parameter σ_0. The Weibull characteristic strength σ_θ, the mean strength $\bar{\sigma}$, or the Weibull material scale factor σ_0, may be scaled to alternative test specimen geometries. Finally, a report citing the original test specimen geometry and strength parameters, as well as the size scaled Weibull strength parameters is prepared.

5. Significance and Use

5.1 Advanced ceramics usually display a linear stress-strain behavior to failure. Lack of ductility combined with flaws that have various sizes and orientations typically leads to large scatter in failure strength. Strength is not a deterministic property but instead reflects the intrinsic fracture toughness and a distribution (size and orientation) of flaws present in the material. This standard is applicable to brittle monolithic ceramics which fail as a result of catastrophic propagation of flaws. Possible rising R-curve effects are also not considered, but are inherently incorporated into the strength measurements.

5.2 Two- and three-parameter formulations exist for the Weibull distribution. This standard is restricted to the two-parameter formulation.

5.3 Tensile and flexural test specimens are the most commonly used test configurations for advanced ceramics. Ring-on-ring and pressure-on-ring test specimens which have multiaxial states of stress are also included. Closed-form solutions for the effective volume and effective surfaces and the Weibull material scale factor are included for these configurations. This practice also incorporates size scaling methods for C-ring test specimens for which numerical approaches are necessary. A generic approach for arbitrary shaped test specimens or components that utilizes finite element analyses is presented in Annex A3.

5.4 The fracture origins of failed test specimens can be determined using fractographic analysis. The spatial distribution of these strength controlling flaws can be over a volume or an area (as in the case of surface flaws). This standard allows for the conversion of strength parameters associated with either type of spatial distribution. Length scaling for strength controlling flaws located along edges of a test specimen is not covered in this practice.

5.5 The scaling of strength with size in accordance with the Weibull model is based on several key assumptions (**5**). It is assumed that the material is uniform, homogeneous, and isotropic. If the material is a composite, it is assumed that the composite phases are sufficiently small that the structure behaves on an engineering scale as a homogeneous and isotropic body. The composite must contain a sufficient quantity of uniformly-distributed, randomly-oriented, reinforcing elements such that the material is effectively homogeneous. Whisker-toughened ceramic composites may be representative of this type of material. This practice is also applicable to composite ceramics that do not exhibit any appreciable bilinear or nonlinear deformation behavior. This standard and the conventional Weibull strength scaling with size may not be suitable for continuous fiber-reinforced composite ceramics. The material is assumed to fracture in a brittle fashion, a consequence of stress causing catastrophic propagation of flaws. The material is assumed to be consistent (batch to batch, day to day, etc.). It is assumed that the strength distribution follows a Weibull two parameter distribution. It is assumed that the same specific flaw type controls strength in the various specimen configurations. It is assumed that each test piece has a statistically significant number of flaws and that they are randomly distributed. It is assumed that the flaws are small relative to the specimen cross section size. If multiple flaw types are present and control strength, then strengths may scale differently for each flaw type. Consult Practice C 1239 and the example in 9.1 for further guidance on how to apply censored statistics in such cases. It is also assumed that the specimen stress state and the maximum stress are accurately determined. It is assumed that the actual data from a set of fractured specimens are accurate and precise. (See Terminology E 456 for definitions of the latter two terms.) For this reason, this standard frequently references other ASTM standard test methods and practices which are known to be reliable in this respect.

5.6 Even if test data has been accurately and precisely measured, it should be recognized that the Weibull parameters determined from test data are in fact estimates. The estimates can vary from the actual (population) material strength parameters. Consult Practice C 1239 for further guidance on the

confidence bounds of Weibull parameter estimates based on test data for a finite sample size of test fractures.

5.7 When correlating strength parameters from test data from one specimen geometry to a second, the accuracy of the correlation depends upon whether the assumptions listed in 5.5 are met. In addition, statistical sampling effects as discussed in 5.6 may also contribute to variations between computed and observed strength-size scaling trends.

5.8 There are practical limits to Weibull strength scaling that should be considered. For example, it is implicitly assumed in the Weibull model that flaws are small relative to the specimen size. Pores that are 50 μm (0.050 mm) in diameter are volume-distributed flaws in tension or flexural strength specimens with 5 mm or greater cross section sizes. The same may not be true if the cross section size is only 100 μm.

6. Probability of Failure Relationships

6.1 *General*:

6.1.1 The random variable representing uniaxial tensile strength of an advanced ceramic will assume only positive values, and the distribution is usually asymmetric about the mean. These characteristics limit the use of the normal distribution (as well as others) and point to the use of the Weibull and similar skewed distributions. Fig. 2 shows the shape of the Weibull distribution as compared to a normal distribution. If the random variable representing uniaxial tensile strength of an advanced ceramic is characterized by a two-parameter Weibull distribution (see Practice C 1239 for a detailed discussion regarding the mathematical description of the Weibull distribution), then the failure probability for a test specimen fabricated from such an advanced ceramic is given by the cumulative distribution function:

$$P_f = 1 - \exp\left[-\left(\frac{\sigma_{max}}{\sigma_\theta}\right)^m\right] \quad \sigma_{max} > 0 \tag{1}$$

$$P_f = 0 \quad \sigma_{max} \leq 0 \tag{2}$$

where:

P_f = the probability of failure,
σ_{max} = maximum tensile stress in a test specimen at failure,
σ_θ = the Weibull characteristic strength (corresponding to a $P_f = 0.632$ or 63.2 %), and
m = Weibull modulus.

6.1.2 As noted earlier, the Weibull characteristic strength is dependent on the test specimen and will change with test specimen geometry as well as the stress state. The Weibull characteristic strength has units of stress, and should be reported using units of MPa or GPa. As was noted in the previous section, strength controlling flaws can be spatially distributed over the volume or the surface (area) of a test specimen. If the strength controlling flaws are volume-distributed, the volume characteristic strength shall be designated as $(\sigma_\theta)_V$, and the volume Weibull modulus shall be designated m_V. If the strength controlling flaws are surface-distributed, the area characteristic strength shall be designated as $(\sigma_\theta)_A$, and the area Weibull modulus shall be designated m_A. Fractographic Practice C 1322 should be used to determine whether flaws are surface- or volume-distributed. It should be borne in mind that a flaw *located* at the surface of a test specimen does not necessarily mean it was a surface-distributed flaw. It may be a surface-distributed flaw, or it may be a volume-distributed flaw which by chance is located at the surface.

6.2 *Volume Distribution*:

6.2.1 An alternative expression for the probability of failure is given by:

$$P_f = 1 - \exp\left[\int_V \left(\frac{\sigma}{(\sigma_0)_V}\right)^{m_V} dV\right] \tag{3}$$

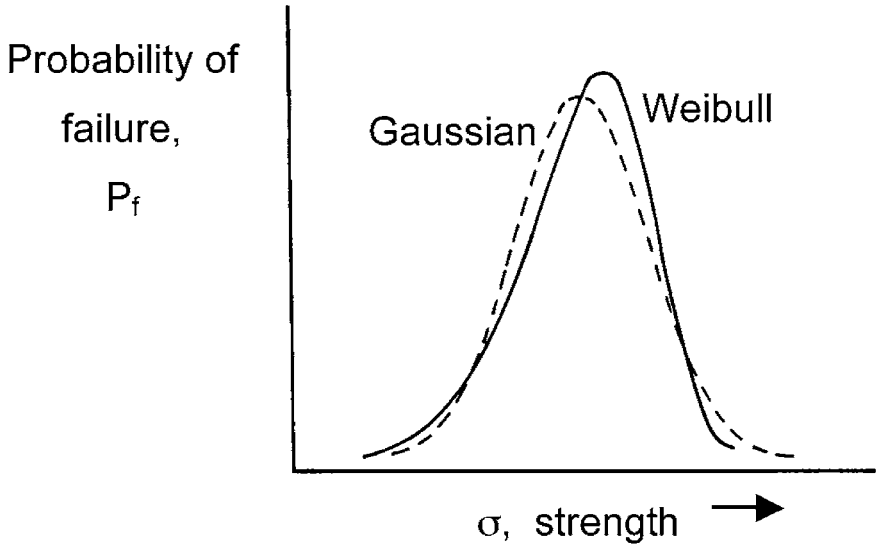

FIG. 2 The Probability Density Function Graphs for Weibull and Gaussian (Normal) Strength Distributions

$$P_f = 0 \quad \sigma \le 0 \tag{4}$$

6.2.1.1 The integration within the exponential function is performed over all tensile stressed regions of the test specimen volume if the strength-controlling flaws are randomly distributed through the volume of the material. m_V is the Weibull modulus associated with strength controlling flaws distributed through the volume. $(\sigma_0)_V$ is the Weibull material scale parameter and can be described as the Weibull characteristic strength of a hypothetical test specimen with unit volume loaded in uniform uniaxial tension. The Weibull material scale parameter has units of stress·(volume)$^{1/m_V}$ and should be reported using units of MPa·(m)$^{3/m_V}$ or GPa·(m)$^{3/m_V}$. Eq 1 and Eq 3 can be equated for a given test specimen geometry, which yields an expression relating $(\sigma_0)_V$ and $(\sigma_\theta)_V$ for that test specimen geometry. Expressions for specific test specimen geometries are presented in Sections 7 and 8.

6.2.2 For the general case where stress varies with position within a test specimen are volume-distributed, the integration given by Eq 3 can be carried out to yield the following expression:

$$P_f = 1 - \exp\left[-kV\left(\frac{\sigma_{max}}{(\sigma_0)_V}\right)^{m_V}\right] \tag{5}$$

6.2.2.1 Here k is a dimensionless factor and has been identified as a "load factor" (e.g., Johnson and Tucker (**6**)). σ_{max} is the maximum stress in the test specimen at failure. Thus, in general:

$$(\sigma_0)_V = (\sigma_\theta)_V\,(kV)^{1/m_V} = (\sigma_\theta)_V\,V_E^{\,1/m_V} \tag{6}$$

when the strength controlling flaws are spatially distributed through the volume. Inclusions are an example of such flaws. For all loading geometries except uniaxial tension (see 7.1), k is a function of the Weibull modulus m and the test geometry. The load factor is evaluated numerically and is always positive and usually less than unity. Notice that the Weibull modulus in this instance, m_V, is associated with volume flaws.

6.2.3 The product k times V is often termed an "effective volume, V_E," in the ceramic literature. The effective volume is the size of a hypothetical tension test specimen that, when stressed to the same level as the test specimen in question, has the same probability of fracture. Expressions for the effective volume of specific test specimen geometries are given Sections 7 and 8. Noting that $(\sigma_0)_V$ is a material parameter (that is in principle independent of the test specimen type), then:

$$(\sigma_0)_V = (\sigma_{\theta,1})_V\,(k_1V_1)^{1/m_V} = (\sigma_{\theta,2})_V\,(k_2V_2)^{1/m_V} \tag{7}$$

where the subscripts 1 and 2 denote two different geometries of test specimens fabricated from the same material. This leads to the following relationship:

$$\frac{(\sigma_{\theta,1})_V}{(\sigma_{\theta,2})_V} = \frac{(k_2V_2)^{1/m_V}}{(k_1V_1)^{1/m_V}} = \left(\frac{k_2V_2}{k_1V_1}\right)^{1/m_V} = \left(\frac{V_{E,2}}{V_{E,1}}\right)^{1/m_V} \tag{8}$$

6.2.3.1 It is implied that the same type of volume-distributed flaws control strength in each geometry. Eq 8 means that knowledge of the effective volume of both specimen types allows the computation of one characteristic strength value based on the characteristic strength value of the other specimen geometry. Test specimens with stress gradients have effective volumes less than the size of the test piece. In other words, $k < 1$. For example, flexural strength specimens expose only a small amount of material to the maximum stress and $k << 1$. The flexure specimen is "equivalent" to a much smaller test piece that is pulled in uniaxial direct tension. The k factors depend upon the geometry and loading configuration and they usually are very sensitive to the Weibull modulus.

6.3 *Surface Distribution*:

6.3.1 If the strength controlling flaws are distributed along the surface of the test specimens, then the following expression:

$$P_f = 1 - \exp\left[\int_A \left(\frac{\sigma}{(\sigma_0)_A}\right)^{m_A} dA\right] \tag{9}$$

$$P_f = 0 \quad \sigma \le 0 \tag{10}$$

shall be utilized for the probability of failure. The integration within the exponential is performed over all tensile regions of the test specimen surface. The integration is sometimes carried out over the area of an effective gage section instead of over the total area of the test specimen. In Eq 9, m_A is the Weibull modulus associated with surface flaws. $(\sigma_0)_A$ is the Weibull material scale parameter and can be described as the Weibull characteristic strength of a test specimen with unit surface area loaded in uniform uniaxial tension. Here the Weibull material scale parameter should be reported using units of MPa·(m)$^{2/m_A}$ or GPa·(m)$^{2/m_A}$. For a given test specimen geometry, Eq 1 and Eq 9 can be equated, which yields an expression relating $(\sigma_0)_A$ and $(\sigma_\theta)_A$. Expressions for specific test specimen geometries are presented in Sections 7 and 8.

6.3.2 For the general case where stress varies within a test specimen and the flaws are surface distributed, the integration given by Eq 3 can be carried out for the surface areas of the specimens that are stressed in tension. This yields the following expression:

$$P_f = 1 - \exp\left[-kA\left(\frac{\sigma_{max}}{(\sigma_0)_A}\right)^{m_A}\right] \tag{11}$$

6.3.2.1 Again, k is a dimensionless factor and has been identified as a "load factor" (e.g., Johnson and Tucker (**6**)). For all loading geometries except uniaxial tension (see 7.1), k is a function of the Weibull modulus m and the test geometry. Notice that the Weibull modulus in this instance, m_A, is associated with surface flaws. σ_{max} is the maximum stress in the test specimen at failure. Thus, in general:

$$(\sigma_0)_A = (\sigma_\theta)_A\,(kA)^{1/m_A} = (\sigma_\theta)_A\,S_E^{\,1/m_A} \tag{12}$$

when the strength controlling flaws are spatially distributed along the surfaces of the test specimens. Surface grinding cracks are an example of such.

NOTE 1—The conventional nomenclature in the literature is used here. *Areas* are denoted by symbols with the letter *A*. The effective area or effective *surface* is commonly denoted by the letter *S*.

6.3.3 For all loading geometries except for uniaxial tension (see 7.2), k is a function of the Weibull modulus m. The load factor, k, is evaluated numerically and is always positive and usually less than unity. In the ceramics literature, the product k times A is often termed an "effective area" or "effective surface, S_E." The effective surface is the size of a hypothetical uniaxial tensile test specimen that, when stressed to the same level as the test specimen in question, has the same probability

of fracture. Expressions for the effective area of specific test specimen geometries are given in Sections 7 and 8. Noting that $(\sigma_0)_A$ is a material parameter (that is in principle independent of the test specimen type), then:

$$\frac{(\sigma_{\theta,1})_A}{(\sigma_{\theta,2})_A} = \frac{(k_2A_2)^{1/m_A}}{(k_1A_1)^{1/m_A}} = \left(\frac{k_2A_2}{k_1A_1}\right)^{1/m_A} = \left(\frac{S_{E,2}}{S_{E,1}}\right)^{1/m_A} \quad (13)$$

where the subscripts 1 and 2 denote two different geometries for test specimens fabricated from the same material. It is implied that the same type of surface-distributed flaws control strength in each geometry. Eq 13 means that knowledge of the effective surfaces of both specimen types allows the computation of one characteristic strength value based on the characteristic strength value of the other specimen geometry. Test specimens with stress gradients have effective surface areas that are less than the size of the test piece and $k < 1$. The flexure specimen is "equivalent" to a smaller test piece that is pulled in uniaxial direct tension. The k factors depend upon the geometry and loading configuration and they usually are very sensitive to the Weibull modulus.

6.4 *Mixed Distributions*:

6.4.1 Strength scaling relations such as Eq 8 and Eq 13 shall not be used to scale strengths where the flaw type in one test specimen type is surface-distributed (e.g., machining cracks) and the flaw type in the second specimen type is volume-distributed (e.g. inclusions), or vice versa. The scaling equations are only suited for cases where the *same* flaw type is active in the two specimen types. For example, if inclusions control strength in specimen type 1, then the scaling may be suitable if inclusions control strength in specimen type 2. If inclusions control strength in specimen type 1, but pores control strength in specimen type 2, then the correlation will probably not be accurate.

6.5 *What May be Scaled*:

6.5.1 Eq 8 and Eq 13 are for scaling the Weibull characteristic strengths, σ_θ, of two different type specimens. The characteristic strengths correspond to a probability of failure, P_f, of 63.2 % for each test specimen set. The equations may also be used to scale strengths at other probabilities of failure, P_f. For example, the median strength ($P_f = 50$ %) of one specimen type can be compared to the median strength of another size or type specimen. Similarly, the strengths at a 1 % probability of failure may be scaled.

NOTE 2—These equations may also be used to scale mean strengths, since they closely approximate the median strengths.

NOTE 3—Scaling predictions or correlations at the 1 % probabilities of failure will be subject to considerable uncertainty, since the confidence intervals for such estimates are much broader than those for the characteristic, median, or mean strengths. It is beyond the scope of this Practice to quantify the confidence intervals for the scaled strengths.

6.6 *Edge-Distributed*:

6.6.1 Weibull edge or length scaling is not covered in this practice. In principle, the same concepts and similar mathematics could be used to scale strengths for edge-distributed flaws, however edge-distributed flaws are often very specific to a particular test specimen type. Edge-distributed flaws are those which form as a result of some process such as chipping, cutting, or grinding and are only found at an edge. Volume or surface type flaws such as pores, inclusions, or normal grinding cracks, which by chance are *located* at a test specimen edge, are not considered edge-distributed flaws. If test specimens have origins that are by nature edge-distributed flaws, the data should be censored as discussed in Practice C 1322 in order to properly analyze the surface- and volume distribution parameters.

7. Test Specimens with Uniaxial Stress States—Effective Volume and Area Relationships

7.1 *Uniaxial Tensile Test Specimens*:

7.1.1 For ambient test temperatures uniaxial tensile test specimens such as shown in Fig. 3 should be tested in accordance with Practice C 1273. For elevated test temperatures tensile test specimens shall be tested in accordance with Test Method C 1366. Various accepted test specimen geometries are presented within these standards. In general, the volume of material subjected to a uniform tensile stress for a single uniaxially-loaded tensile test specimen may be many times that of a single flexural test specimen. Strength values obtained using the different recommended tensile test specimens (Practice C 1273 or Test Method C 1366) with different volumes (areas) of material will be different due to these volume (area) differences. Characteristic or mean strength values can be scaled to any gage section and to other test configurations using the volume and area relationships presented in this section, which are applicable to the test specimen geometries presented in Practice C 1273 and Test Method C 1366.

7.1.2 *Volume Distribution*—The relationship between the characteristic strength $(\sigma_{\theta T})_V$ and the Weibull material scale parameter $(\sigma_0)_V$ for a tension test specimen with volume flaws is:

$$(\sigma_0)_V = (\sigma_{\theta T})_V \, V_T^{1/m_V} \quad (14)$$

7.1.2.1 This expression is obtained by setting Eq 1 equal to Eq 3, after the integration in Eq 3 has been performed over the gage section volume of the uniaxial tensile test specimen. Thus V_T is the volume of the gage section. Comparison of Eq 14 with Eq 6 yields the following formulation for the effective volume:

$$V_E = kV = V_T \quad (15)$$

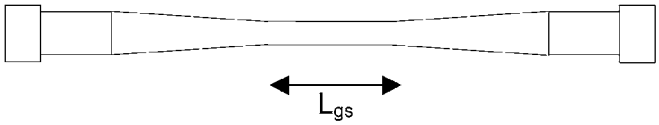

NOTE—L_{gs} is the length of the gage section.

FIG. 3 Example of a Round Tension Strength Specimen

7.1.2.2 Thus, for uniaxial tension, k is equal to unity. An expression (**7**) similar to Eq 14 can be derived relating the material scale parameter to the average uniaxial tensile strength, that is:

$$(\sigma_0)_V = \frac{(\bar{\sigma}_T)_V V_T^{1/m_V}}{\Gamma\left[\frac{1}{m_V} + 1\right]} \quad (16)$$

NOTE 4—Ideally the tapered regions at the end of a gage section should be included in the volume, but their contribution to the effective volume usually is relatively small compared to the gage section. They therefore are omitted here for simplicity.

NOTE 5—The gamma function in the denominator may be found in any handbook on mathematical functions.

7.1.2.3 The procedure in 7.1.2 is an approximation that does not include the tapered portions of the test piece on either side of the gage section. Hence, k and V_E are underestimated by a small amount. Better estimates of k and the effective volume should be obtained by numerical analysis as discussed in Annex A3.

7.1.3 *Surface Distribution*—The following equation defines the relationship between the characteristic strength and the material scale parameter for a tension test specimen with surface flaws is:

$$(\sigma_0)_A = (\sigma_{\theta T})_A A_T^{1/m_A} \quad (17)$$

7.1.3.1 This expression is obtained by Eq 1 and Eq 9, after the integration in Eq 9 has been performed over the gage section area of the uniaxial tensile test specimen. A_T is the area of the gage section. Comparison of Eq 17 with Eq 12 yields the following formulation for the effective area:

$$S_E = kA = A_T \quad (18)$$

7.1.3.2 Thus for uniaxial tension k is equal to unity. An expression similar to Eq 17 can be derived relating the material scale parameter to the average uniaxial tensile strength, that is:

$$(\sigma_0)_A = \frac{(\bar{\sigma}_T)_A A_T^{1/m_A}}{\Gamma\left[\frac{1}{m_A} + 1\right]} \quad (19)$$

NOTE 6—Ideally the tapered regions at the end of a gage section should be included in the area, but their contribution to the effective area usually is relatively small compared to the gage section. They therefore are omitted here for simplicity.

7.1.3.3 The procedure in 7.1.3 is an approximation and does not include the portions of the test piece on either side of the gage section. Hence, k and S_E are underestimated by a small amount. Improved estimates of k and S_E should be obtained by numerical analysis as discussed in Annex A3.

7.1.4 No adjustments are made to the volume or surface integrals for the presence of chamfers or edge rounding in square or rectangular cross section tension specimens. This is an acceptable approximation provided that the chamfer and rounding sizes are small. See section 6.6 if origins are on the specimen edges.

7.2 *Rectangular Flexure Test Specimens*:

7.2.1 For ambient test temperatures, flexure test specimens with rectangular cross sections such as shown in Fig. 4 should be tested in three- or four-point flexure in accordance with Test Method C 1161. For elevated test temperatures, flexure test specimens should be tested in accordance with Test Method C 1211. Since volume and/or surface effects will affect strength values, then the strength values obtained using bend bars with different sizes and loading configurations (e.g., three-point, ¼-point four-point, or ⅓-point 4-point) will vary. Characteristic or mean strength values can be scaled to other test specimen geometries using the volume and area relationships presented in this section.

7.2.2 *Volume Distribution*—For flexural test specimen geometries, the strength relationships become more complex due to the nonuniform stress state (**8, 9**). The stress state is primarily uniaxial, however. For four-point flexure test specimens, the gage volume within the outer supporting points V_{B4} is given by:

$$V_{B4} = bdL_{o4} \quad (20)$$

where b and d are dimensions identified in Fig. 4. One half of this gage volume is stressed in tension. The relationship between the characteristic strength $(\sigma_{\theta B4})_V$ and the Weibull material scale parameter $(\sigma_0)_V$ for a rectangular flexure specimen with volume flaws is (**8, 9**):

$$(\sigma_0)_V = (\sigma_{\theta B4})_V \left\{\left[\left(\frac{L_{i4}}{L_{o4}}\right)(m_V) + 1\right]\left[\frac{1}{2(m_V + 1)^2}\right] V_{B4}\right\}^{1/m_V} \quad (21)$$

which relates the Weibull characteristic strength $(\sigma_\theta)_V$ to the Weibull material scale parameter $(\sigma_0)_V$

where:

L_{i4} = length of inner span identified in Fig. 4, and
L_{o4} = length of outer span identified in Fig. 4.

7.2.2.1 Eq 21 is obtained by setting Eq 1 equal to Eq 3, after the integration in Eq 3 has been performed over the gage section volume of the flexure test specimen. Comparing Eq 21 with Eq 6 yields the following formulation for the effective volume:

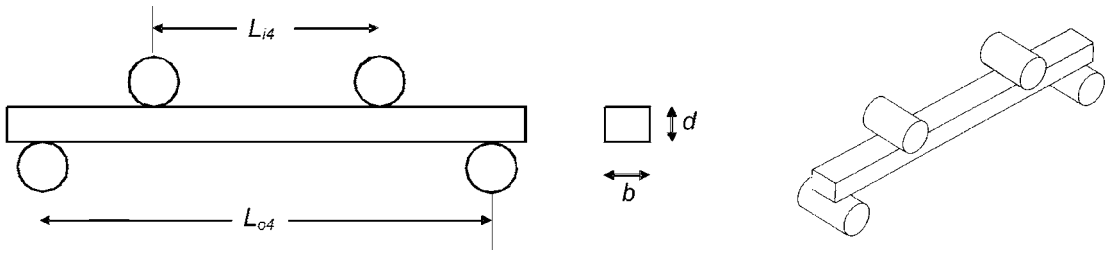

NOTE—The four-point configuration is shown.

FIG. 4 Typical Flexural Strength Test Specimen Geometry

$$V_E = kV_{B4} = \left[\left(\frac{L_{i4}}{L_{o4}}\right)(m_V) + 1\right]\left[\frac{1}{2(m_V+1)^2}\right]V_{B4} \quad (22)$$

7.2.2.2 For specific flexural strength configurations the above formula simplifies considerably. For example, for ¼-point, 4-point loading as specified in Test Methods C 1161 and C 1211:

$$V_E = kV_{B4} = \frac{(m_V+2)}{4(m_V+1)^2}V_{B4} \quad (23)$$

7.2.2.3 For the general four-point configuration, the relationship between the mean flexure strength ($\bar{\sigma}_{B4}$) and the Weibull material scale parameter $(\sigma_0)_V$ is:

$$(\sigma_0)_V = \frac{(\bar{\sigma}_{B4})_V\left\{\left[\left(\frac{L_{i4}}{L_{o4}}\right)(m_V)+1\right]\left[\frac{1}{2(m_V+1)^2}\right]V_B\right\}^{1/m_V}}{\Gamma\left(\frac{1}{m_V}+1\right)} \quad (24)$$

7.2.3 *Surface Distribution*—The total gage area within the outer supporting points A_{B4} for four-point loading is given by:

$$A_{B4} = 2L_{o4}(b+d) \quad (25)$$

7.2.3.1 Only half of this area is stressed in tension. The relationship between the characteristic strength $(\sigma_{\theta B4})_A$ and the Weibull material scale parameter $(\sigma_0)_A$ for rectangular flexure specimens with surface flaws is:

$$(\sigma_0)_A = (\sigma_{\theta B4})_A\left\{L_{o4}\left[\frac{d}{(m_A+1)}+b\right]\left[\left(\frac{L_{i4}}{L_{o4}}\right)m_A+1\right]\left[\frac{1}{(m_A+1)}\right]\right\}^{1/m_A} \quad (26)$$

7.2.3.2 This expression is obtained by Eq 1 and Eq 9 after the integration in Eq 9 has been performed over the gage section area of the flexure specimen. This integration includes both the bottom tensile surface as well as the portions of the side surfaces that are stressed in tension. Comparing Eq 26 with Eq 12 yields the following formulation for the effective area:

$$S_E = kA_{B4} = L_{o4}\left[\frac{d}{(m_A+1)}+b\right]\left[\left(\frac{L_{i4}}{L_{o4}}\right)m_A+1\right]\left[\frac{1}{(m_A+1)}\right] \quad (27)$$

7.2.3.3 The average flexure strength $(\bar{\sigma}_{B4})_A$ is related to the Weibull material scale parameter $(\sigma_0)_A$:

$$(\sigma_0)_A = \frac{(\bar{\sigma}_{B4})_A\left\{L_{o4}\left[\frac{d}{m_A+1}+b\right]\left[\left(\frac{L_{i4}}{L_{o4}}\right)m_A+1\right]\left[\frac{1}{m_A+1}\right]\right\}^{1/m_A}}{\Gamma\left(\frac{1}{m_A}+1\right)} \quad (28)$$

7.2.4 *Three-Point Flexure*—The Weibull material scale parameter, and the effective volumes and effective areas of rectangular cross sectional beams in three-point bending can be obtained by simply setting $L_{i4} = 0$, and using L_{o3} in place of L_{o4} in Eq 21, Eq 22, Eq 24, Eq 27, and Eq 28.

7.2.5 Stress scaling ratios for flexural strength specimens of various types usually depend upon whether the flaws are surface- or volume-distributed. An important exception is for flexural strength test specimens of *identical* cross section size (**9**). The strength scaling between any two flexural loadings are the same, irrespective of whether volume or surface scaling is used. For example, the relationship of the characteristic strengths of three-point and four-point flexure strengths for *either* volume or surface flaws is:

$$\frac{\sigma_{\theta B3}}{\sigma_{\theta B4}} = \left(\frac{L_{o4}}{L_{o3}}\right)^{1/m}\left(\frac{m+2}{2}\right)^{1/m} \quad (29)$$

7.2.5.1 This is true only if both sets break from volume flaws (or alternatively both sets from surface flaws). The mean strengths also scale according to Eq 29.

7.2.6 No adjustments are made to the volume or surface integrals for the presence of chamfers or edge rounding in flexure specimen. This is an acceptable approximation provided that the chamfer and rounding sizes are small. See section 6.6 if origins are on the specimen edges.

7.3 *Round Flexural Strength Specimens*:

7.3.1 Round rods such as shown in Fig. 5 may be tested by any flexural testing procedure provided that it produces accurate and precise strength data. The strength values obtained using round rods with different sizes and loading configurations (e.g., three-point, ¼-point four-point, or ⅓-point 4-point) will vary. Characteristic or mean strength values can be scaled to other test specimen geometries using the volume and area relationships presented in this section.

7.3.2 *Volume Distribution*—For round flexure test specimens, the gage volume within the outer supporting points V_B is given by:

$$V_{B4} = \pi D^2 L_{o4}/4 \quad (30)$$

where dimensions are identified in Fig. 5. Only half of this gage volume is stressed in tension. The relationship between the characteristic strength $(\sigma_{\theta B4})_V$ and the Weibull material scale parameter $(\sigma_0)_V$ for round four-point flexure specimens with volume flaws is (**10**):

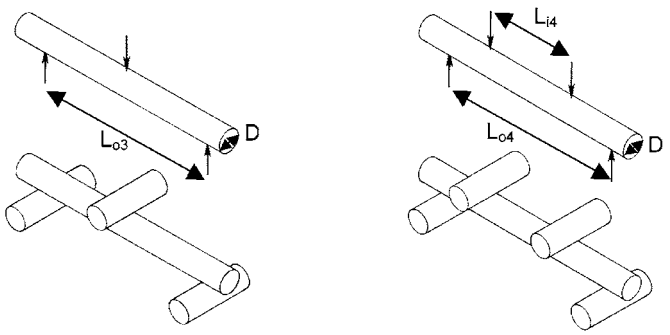

FIG. 5 Round Flexural Strength Test Geometry

$$(\sigma_0)_V = (\sigma_{\theta B4})_V \left\{ \left[\left(\frac{L_{i4}}{L_{o4}} \right) (m_V) + 1 \right] \left[\frac{1}{m_V + 1} \right] \left(\frac{G}{\pi} \right) V_{B4} \right\}^{1/m_V} \tag{31}$$

where:

L_{i4} = length of inner span identified in Fig. 4,
L_{o4} = length of outer span identified in Fig. 4, and
G = a combined gamma function given by:

$$G = \left(\frac{\Gamma\left(\frac{m+1}{2}\right) \Gamma\left(\frac{3}{2}\right)}{\Gamma\left(\frac{m+4}{2}\right)} \right) \tag{32}$$

7.3.2.1 G is shown in Annex A1 for typical values of Weibull moduli. Eq 31 is obtained by setting Eq 1 equal to Eq 3, after the integration in Eq 3 has been performed over the gage section volume of the round flexure specimen. Comparing Eq 31 with Eq 6 yields the following formulation for the effective volume:

$$V_E = kV_{B4} = \left[\left(\frac{L_{i4}}{L_{o4}} \right) (m_V) + 1 \right] \left[\frac{1}{(m_V + 1)} \right] \left(\frac{G}{\pi} \right) V_{B4} \tag{33}$$

7.3.2.2 For specific flexural strength configurations the above formula simplifies considerably. For example for ¼-point, 4-point loading:

$$V_E = kV_{B4} = \frac{(m_V + 2)}{2(m_V + 1)} \left(\frac{G}{\pi} \right) V_{B4} \tag{34}$$

7.3.2.3 For the general case of 4-point loading, the relationship between the mean flexure strength ($\bar{\sigma}_{B4}$) and the Weibull material scale parameter $(\sigma_0)_V$ is:

$$(\sigma_0)_V = \frac{(\bar{\sigma}_{B4})_V \left\{ \left[\left(\frac{L_{i4}}{L_{o4}} \right) (m_V) + 1 \right] \left[\frac{1}{(m_V + 1)} \right] V_{B4} \right\}^{1/m_V}}{\Gamma\left(\frac{1}{m_V} + 1 \right)} \tag{35}$$

7.3.3 *Surface Distribution*—The total gage area within the outer supporting points A_{B4} for four-point loading is given by:

$$A_{B4} = L_{o4} (\pi D) \tag{36}$$

7.3.3.1 Only half of this area is stressed in tension. The relationship between the characteristic strength $(\sigma_{\theta B4})_A$ and the Weibull material scale parameter $(\sigma_0)_A$ for a round flexure specimen with surface flaws is:

$$(\sigma_0)_A = (\sigma_{\theta B4})_A \left\{ \left[\left(\frac{L_{i4}}{L_{o4}} \right) (m_A) + 1 \right] \left[\frac{(m_A + 2)}{2} \right] \left[\frac{1}{(m_A + 1)} \right] \left(\frac{G}{\pi} \right) A_{B4} \right\}^{1/m_V} \tag{37}$$

which relates the Weibull characteristic strength $(\sigma_\theta)_A$ to the Weibull material scale parameter $(\sigma_0)_A$. Comparing Eq 37 with Eq 12 yields the following formulation for the effective area:

$$S_E = kA_{B4} = \left[\left(\frac{L_{i4}}{L_{o4}} \right) m_A + 1 \right] \left[\frac{(m_A + 2)}{2} \right] \left[\frac{1}{(m_A + 1)} \right] \left(\frac{G}{\pi} \right) A_{B4} \tag{38}$$

7.3.3.2 This expression is obtained by Eq 1 and Eq 9, after integration in Eq 9 has been performed over the gage section area of the flexure bar. For specific flexural strength configurations the above formula simplifies considerably. For example, for ¼-point, 4-point loading:

$$S_E = kA_{B4} = \frac{(m_A + 2)^2}{4(m_A + 1)} \left(\frac{G}{\pi} \right) A_{B4} \tag{39}$$

7.3.3.3 For the general case of 4-point loading, the average flexure strength ($\bar{\sigma}_{B4}$) is related to the Weibull material scale parameter $(\sigma_0)_A$:

$$(\sigma_0)_A = \frac{(\bar{\sigma}_{B4})_A \left\{ \left[\left(\frac{L_{i4}}{L_{o4}} \right) m_A + 1 \right] \left[\frac{(m_A + 2)}{2} \right] \left[\frac{1}{(m_A + 1)} \right] \left(\frac{G}{\pi} \right) A_{B4} \right\}^{1/m_A}}{\Gamma\left(\frac{1}{m_A} + 1 \right)} \tag{40}$$

7.3.4 The Weibull material scale parameter, and the effective volume and effective area of round rods in three-point bending can be obtained by simply setting $L_{i4} = 0$, and using L_{o3} in place of L_{o4} in Eq 31, Eq 33, Eq 35, Eq 37, and Eq 38.

7.3.5 Stress scaling ratios for flexural strength specimens of various types *usually* depend upon whether the flaws are surface- or volume-distributed. An important exception is round flexural strength specimens with identical diameters (**10**). The strength scaling between *any* two flexural loadings are the same irrespective of whether volume or surface scaling is used. For example, the relationship of the characteristic strengths (or mean strengths) of three-point and four-point flexure strengths for *either* volume or surface flaws is:

$$\frac{\sigma_{\theta B3}}{\sigma_{\theta B4}} = \left(\frac{L_{B4}}{L_{B3}} \right)^{1/m} \left(\frac{m+2}{2} \right)^{1/m} \tag{41}$$

7.3.5.1 This is true only if both sets break from volume flaws (or alternatively both sets from surface flaws). The mean strengths also scale according to Eq 41.

NOTE 7—This is the same outcome as for rectangular test specimens in 7.2.5.

7.4 *C-Ring Test Specimens*:

7.4.1 C-ring test specimens such as shown in Fig. 6 shall be tested in diametral compression in accordance with Test Method C 1323. The strength values obtained using C-ring test specimens with different sizes will vary. Characteristic or mean strength values can be scaled to other test specimen geometries using the volume and area relationships presented in this section.

7.4.2 *Volume Distribution*—The gage section volume for a C-ring specimen is:

$$V_{CR} = \pi (r_o^2 - r_i^2) b / 2 \tag{42}$$

7.4.2.1 This is the volume of the C-ring on the right hand side of Fig. 6 between the top and bottom loading points. The relationship between the characteristic strength $(\sigma_{\theta CR})_V$ and the Weibull material scale parameter $(\sigma_0)_V$ for a C-ring test specimen with volume flaws is (**11**):

$$(\sigma_0)_V = (\sigma_{\theta CR})_V \left[(r_o)^{m_V} f(\theta) f(r) \right]^{1/m_V} \tag{43}$$

where:

$$f(\theta) = \sqrt{\pi} \left[\frac{\Gamma\left(\frac{m_V + 1}{2} \right)}{\Gamma\left(\frac{m_V}{2} + 1 \right)} \right] \tag{44}$$

$$f(r) = 2 \int_{r_a}^{r_o} \left(\frac{r - r_a}{r_o - r_a} \right)^{m_V} r^{(1 - m_V)} dr \tag{45}$$

where $r_a = (r_o - r_i)/2$. The expression in Eq 43 is obtained by setting Eq 1 equal to Eq 3, after the integration in Eq 3 has been

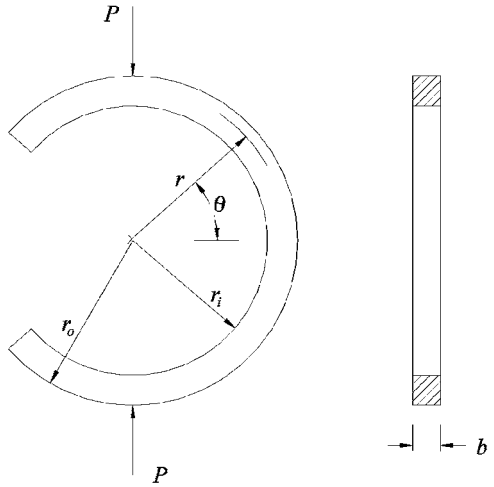

FIG. 6 Typical Compression C-Ring Test Specimen Geometry

performed over the gage section volume of the C-ring test specimen. Comparison of Eq 43 with Eq 6 yields the following formulation for the effective volume:

$$V_E = kV_{CR} = (r_o)^{m_V} f(\theta) f(r) \tag{46}$$

7.4.2.2 This equation also must be solved by numerical means since a closed form solution does not as yet exist. For C-ring specimens, the average strength $(\bar{\sigma}_{CR})_V$ is related to the Weibull material scale parameter, $(\sigma_0)_V$:

$$(\sigma_0)_V = \frac{(\bar{\sigma}_{CR})_V \left[(r_o)^{m_V} f(\theta) f(r)\right]^{1/m_V}}{\Gamma\left[\frac{1}{m_V} + 1\right]} \tag{47}$$

7.4.3 *Surface Distribution*—The relationship between the characteristic strength $(\sigma_{\theta CR})_A$ and the Weibull material scale parameter $(\sigma_0)_A$ for a C-ring specimen with surface flaws is (**11**):

$$(\sigma_0)_A = (\sigma_{\theta CR})_A \left[b\, r_o f(\theta) + 2(r_o)^{m_A} f(\theta)\, f(r)\right]^{1/m_A} \tag{48}$$

7.4.3.1 This expression is obtained by Eq 1 and Eq 9, after the integration in Eq 9 has been performed over the gage section area of the C-ring test specimen. The gage section area is the area of the C-ring on the right hand side of Fig. 6 between the top and bottom loading points. It includes the front and back face surfaces between these two locations as well as the outer curved surface area. Eq 48 must be solved by numerical means since a closed form solution does not as yet exist. Comparison of Eq 48 with Eq 12 yields the following formulation for the effective surface (effective area):

$$S_E = kA_{CR} = b\, r_o f(\theta) + 2r_o^{m_A} f(\theta)\, f(r) \tag{49}$$

7.4.3.2 This equation must be solved by numerical means since a closed form solution does not as yet exist. For C-ring specimens, the average strength $(\bar{\sigma}_{CR})_A$ is related to the Weibull material scale parameter, $(\sigma_0)_A$:

$$(\sigma_0)_A = \frac{(\bar{\sigma}_{CR})_A \left[b\, r_o f(\theta) + 2(r_o)^{m_A} f(\theta)\, f(r)\right]^{1/m_A}}{\Gamma\left[\frac{1}{m_A} + 1\right]} \tag{50}$$

7.4.4 No adjustments are made to the volume or surface integrals for the presence of chamfers or edge rounding in C-ring specimen, if such exist. This is an acceptable approximation provided that the chamfer and rounding sizes are small. See section 6.6 if origins are on the specimen edges.

8. Test Specimens with Multiaxial Stress States—Effective Volume and Area Relationships

8.1 *Pressure-on-Ring Test Specimens*:

8.1.1 Pressure-on-ring (POR) test specimens such as shown in Fig. 7 shall be tested in accordance with any procedure provided that it produces accurate and precise strength data. The strength values obtained using different sized specimens will vary. Characteristic or mean strength values can be scaled to other test specimen geometries using the volume and area relationships presented in this section.

8.1.2 *Volume Distribution*—The stress state is primarily equibiaxial in the middle, but mixed radial and hoop tension away from the middle out to the support ring. The pressurize-on-ring disk gage volume is the volume of the disk test specimen within the support ring:

$$V_{POR} = \pi R_S^2 h \tag{51}$$

where h is the disk thickness and R_S is the support ring radius. The relationship between the characteristic strength $(\sigma_{\theta POR})_V$ and the Weibull material scale parameter $(\sigma_0)_V$ for a pressure-on-ring test specimen with volume flaws is (**12**):

$$(\sigma_0)_V = \tag{52}$$
$$(\sigma_{\theta POR})_V \left\{ \left\{ \frac{4\pi(1+\nu)}{1+m_V} \left(\frac{R_S}{R_d}\right)^2 \left[\frac{2R_d^2(1+\nu) + R_S^2(1-\nu)}{(3+\nu)(1+3\nu)} \right] \right\} \left\{ \frac{h}{2(m_V+1)} \right\} \right\}^{1/m_V}$$

where:

R_S = the support ring radius, and

ν = Poisson's ratio.

8.1.2.1 The expression in Eq 52 is based on the Principal Independent Action (PIA) model (**12, 13**) for the effect of multiple tension stresses on a material element.

NOTE 8—The PIA model simply assumes that each principal stress contributes independently to the risk of rupture for each volume or area sub element in a body. See Annex A2.

8.1.2.2 Comparing Eq 52 with Eq 6 yields the following formulation for the effective volume:

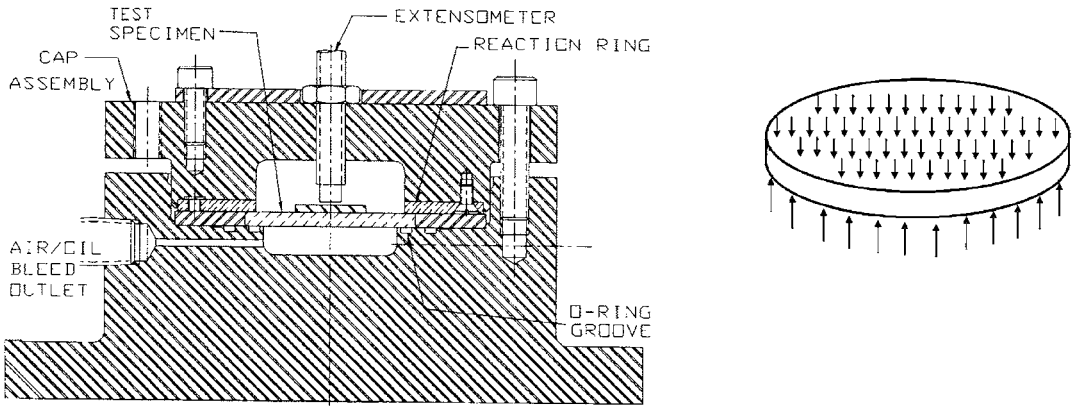

FIG. 7 Pressure-on-Ring Test Specimen Geometry (from Salem and Adams) (12)

$$V_E = kV_{POR} = \left[\frac{4\pi(1+\nu)}{1+m_V}\left(\frac{R_s}{R_d}\right)^2\left[\frac{2R_d^2(1+\nu)+R_s^2(1-\nu)}{(3+\nu)(1+3\nu)}\right]\left\{\frac{h}{2(m_V+1)}\right\}\right] \quad (53)$$

8.1.2.3 For pressure-on-ring disk specimens, the average strength $(\bar{\sigma}_{POR})_V$ is related to the Weibull material scale parameter, $(\sigma_0)_V$:

$$(\sigma_0)_V = \frac{(\bar{\sigma}_{POR})_V\left\{\left[\frac{4\pi(1+\nu)}{1+m_V}\right]\left(\frac{R_s}{R_d}\right)^2\left[\frac{2R_d^2(1+\nu)+R_s^2(1-\nu)}{(3+\nu)(1+3\nu)}\right]^2\left\{\frac{h}{2(m_V+1)}\right\}\right\}^{1/m_V}}{\Gamma\left[\frac{1}{m_V}+1\right]} \quad (54)$$

8.1.3 *Surface Distribution*—The gage area of a pressure-on-ring test specimen is the circular surface area within the support ring:

$$A_{POR} = \pi R_s^2 \quad (55)$$

8.1.3.1 The relationship between the characteristic strength $(\sigma_{\theta B4})_A$ and the Weibull material scale parameter $(\sigma_0)_A$ for a pressure-on-ring specimen with surface flaws is (**12**):

$$(\sigma_0)_A = (\sigma_{\theta POR})_A\left\{\frac{4\pi(1+\nu)}{1+m_A}\left(\frac{R_s}{R_d}\right)^2\left[\frac{2R_d^2(1+\nu)+R_s^2(1-\nu)}{(3+\nu)(1+3\nu)}\right]\right\}^{1/m_A} \quad (56)$$

8.1.3.2 Eq 56 is obtained by setting Eq 1 equal to Eq 9, after the integration in Eq 9 has been performed over the gage section area of the pressure-on-ring test specimen, assuming a principle of independent action (PIA) reliability model. Comparison of Eq 56 with Eq 12 yields the following formulation for the effective surface effective area:

$$S_E = kA_{POR} = \frac{4\pi(1+\nu)}{1+m_A}\left(\frac{R_s}{R_d}\right)^2\left[\frac{2R_d^2(1+\nu)+R_s^2(1-\nu)}{(3+\nu)(1+3\nu)}\right] \quad (57)$$

8.1.3.3 The material scale parameter is related to the average pressure-on-ring disk strength by:

$$(\sigma_0)_A = \frac{(\bar{\sigma}_{POR})_A\left\{\frac{4\pi(1+\nu)}{1+m_A}\left(\frac{R_s}{R_d}\right)^2\left[\frac{2R_d^2(1+\nu)+R_s^2(1-\nu)}{(3+\nu)(1+3\nu)}\right]\right\}^{1/m_A}}{\Gamma\left[\frac{1}{m_A}+1\right]} \quad (58)$$

8.2 *Ring-on-Ring Test Specimens*:

8.2.1 Ring-on-ring test specimens such as shown in Fig. 8 shall be tested in accordance with Test Method C 1499. The strength values obtained using ring-on-ring specimens vary with test specimen size. Characteristic or mean strength values can be scaled to other test specimen geometries using the volume and area relationships presented in this section. The analysis is based on a Principal Independent Action (PIA) model for the contribution of the multiple stresses acting on any element of the material (**13, 14**).

NOTE 9—The PIA model simply assumes that each principal stress

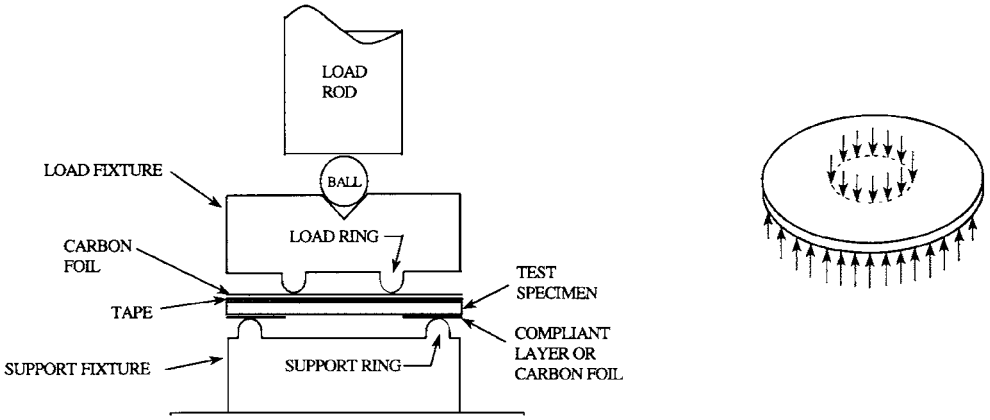

FIG. 8 Ring-on-Ring Test Specimen Geometry from Test Method C 1499

contributes independently to the risk of rupture for each volume or area sub element in a body. See Annex A2.

8.2.2 *Volume Distribution*—The gage volume of a ring-on-ring test specimen is the volume of the disk within the support ring:

$$V_{ROR} = \pi D_s^2 h / 4 \tag{59}$$

8.2.2.1 About half of this volume is under tensile stress. The relationship between the characteristic strength $(\sigma_{\theta ROR})_V$ and the Weibull material scale parameter $(\sigma_0)_V$ for a ring-on-ring test specimen with volume flaws, from Test Method C 1499 and Ref **(14)** is:

$$(\sigma_0)_V = \tag{60}$$
$$(\sigma_{\theta ROR})_V \left\{\frac{\pi}{2}D_L^2\right\}^{1/m_V}\left\{\left\{1+\left[\frac{44(1+\nu)}{3(1+m_V)}\right]\left[\frac{5+m_V}{2+m_V}\right]\left(\frac{D_S-D_L}{D_S D}\right)^2\left[\frac{2D^2(1+\nu)+(D_S-D_L)^2(1-\nu)}{(3+\nu)(1+3\nu)}\right]\right\}\left\{\frac{h}{2(m_V+1)}\right\}\right\}^{1/m_V}$$

where:

D_L = loading ring diameter,
D_S = support ring diameter,
D = overall disk diameter,
h = disk thickness, and
ν = Poisson's ratio.

8.2.2.2 Note that the outer diameter of the disk, D plays a role as well as the inner loading diameter, D_L, and the outer support ring diameter, D_S. Note also that, in this case, the second term on the right is not V_{ROR}. Portions of the third and fourth terms on the right contribute to V_{ROR}. Eq 60 is obtained by setting Eq 1 equal to Eq 3, after the integration in Eq 3 has been performed over the gage section volume of the ring-on-ring test specimen, assuming a principle of independent action (PIA) reliability model. Comparison of Eq 60 with Eq 6 yields the following formulation for the effective volume:

$$V_E = kV_{ROR} = \tag{61}$$
$$\left\{\frac{\pi}{2}D_L^2\right\}\left\{1+\left[\frac{44(1+\nu)}{3(1+m_V)}\right]\left[\frac{5+m_V}{2+m_V}\right]\left(\frac{D_S-D_L}{D_S D}\right)^2\left[\frac{2D^2(1+\nu)+(D_S-D_L)^2(1-\nu)}{(3+\nu)(1+3\nu)}\right]\right\}\left\{\frac{h}{2(m_V+1)}\right\}$$

8.2.2.3 Note again that the first term on the right is only a portion of V_{ROR}. For ring-on-ring disk specimens, the average strength $(\bar{\sigma}_{ROR})_V$ is related to the Weibull material scale parameter, $(\sigma_0)_V$:

$$(\sigma_0)_V = \tag{62}$$
$$\frac{(\bar{\sigma}_{ROR})_V\left[\left\{\frac{\pi}{2}D_L^2\right\}\left\{1+\left[\frac{44(1+\nu)}{3(1+m_V)}\right]\left[\frac{5+m_V}{2+m_V}\right]\left(\frac{D_S-D_L}{D_S D}\right)^2\left[\frac{2D^2(1+\nu)+(D_S-D_L)^2(1-\nu)}{(3+\nu)(1+3\nu)}\right]\right\}\left\{\frac{h}{2(m_V+1)}\right\}\right]^{1/m_V}}{\Gamma\left[\frac{1}{m_V}+1\right]}$$

8.2.3 *Surface Distribution*—The gage area of a ring-on-ring test specimen is the circular area of the disk within the support ring:

$$A_{ROR} = \pi D_S^2 / 4 \tag{63}$$

8.2.3.1 The relationship between the characteristic strength $(\bar{\sigma}_{ROR})_A$ and the Weibull material scale parameter $(\sigma_0)_A$ for a ring-on-ring test specimen with volume flaws, from Test Method C 1499 and Ref **(14)** is:

$$(\sigma_0)_V = \tag{64}$$
$$(\sigma_{\theta ROR})_V \left\{\frac{\pi}{2}D_L^2\right\}^{1/m_A}\left\{\left[1+\left[\frac{44(1+\nu)}{3(1+m_A)}\right]\left[\frac{5+m_A}{2+m_A}\right]\left(\frac{D_S-D_L}{D_S D}\right)^2\left[\frac{2D^2(1+\nu)+(D_S-D_L)^2(1-\nu)}{(3+\nu)(1+3\nu)}\right]\right]\right\}^{1/m_A}$$

8.2.3.2 Eq 64 is obtained by setting Eq 1 equal to Eq 9, after the integration in Eq 9 has been performed over the gage section area of the ring-on-ring test specimen, assuming a principle of independent action (PIA) reliability model. Comparison of Eq 64 with Eq 12 yields the following formulation for the effective surface (effective area):

$$S_E = kA_{ROR} = \tag{65}$$
$$\frac{\pi}{2}D_L^2\left\{1+\left[\frac{44(1+\nu)}{3(1+m_A)}\right]\left[\frac{5+m_A}{2+m_A}\right]\left(\frac{D_S-D_L}{D_S D}\right)^2\left[\frac{2D^2(1+\nu)+(D_S-D_L)^2(1-\nu)}{(3+\nu)(1+3\nu)}\right]\right\}$$

8.2.3.3 The material scale parameter is related to the average ring-on-ring disk strength by:

$$(\sigma_0)_A = \tag{66}$$
$$\frac{(\bar{\sigma}_{ROR})_A\left[\frac{\pi}{2}D_L^2\left\{1+\left[\frac{44(1+\nu)}{3(1+m_A)}\right]\left[\frac{5+m_A}{2+m_A}\right]\left(\frac{D_S-D_L}{D_S D}\right)^2\left[\frac{2D^2(1+\nu)+(D_S-D_L)^2(1-\nu)}{(3+\nu)(1+3\nu)}\right]\right\}\right]^{1/m_A}}{\Gamma\left[\frac{1}{m_A}+1\right]}$$

9. Examples—Converting Characteristic Strengths

9.1 *Example—Converting Characteristic Strengths: Uniaxial Tensile Test Specimens*:

9.1.1 Consider the tensile strength data from Ref **(15)** listed in Table 1. The material is a silicon nitride monolithic ceramic that has multiple flaw populations. The treatment of the multiple flaw populations follows the procedures specified in Practice C 1239 and Ref **(16)**. The test specimen geometry (developed at Oak Ridge National Laboratory (ORNL, Ref **(17)**) is given in Fig. 9.

9.1.2 The failure origin for each test specimen was identified as either a volume or a surface fracture origin, and parameter estimates were obtained by using maximum likelihood estimators in a manner outlined in Practice C 1239. For this data the analysis yielded values of $(\hat{m})_a = 6.66$ and $(\hat{\sigma}_\theta)_a =$ 787 MPa. (The symbol "^" over the stress terms denotes that these are estimates of the population parameters as per guidelines in Practice C 1239.) Focusing on the surface flaw parameters and utilizing Eq 19 with $A_T = 330$ mm^2, then $\hat{\sigma}_0)_a =$ 1881 MPa·(mm)$^{0.30}$ or 237 MPa·(m)$^{0.30}$. With only two volume outcomes, no meaningful estimate of the Weibull volume parameters can be made.

9.1.3 The area strength values (characteristic and/or mean strengths) can be scaled to any gage section using the area relationships presented earlier. A B-size ¼-point four-point flexural test specimen in Test Method C 1161 (3 mm by 4 mm by 40+ mm) would have an effective area of 99.3 mm^2 (from Eq 27). The surface area strength parameters obtained from the

TABLE 1 Silicon Nitride Failure Data—Ref (15)

Test Specimen Number	Failure Stress (MPa)	Fracture Origin
1	570	Surface
2	579	Surface
3	633	Surface
4	626	Surface
5	641	Volume
6	683	Surface
7	726	Surface
8	722	Surface
9	741	Surface
10	811	Volume
11	813	Surface
12	852	Surface
13	958	Surface

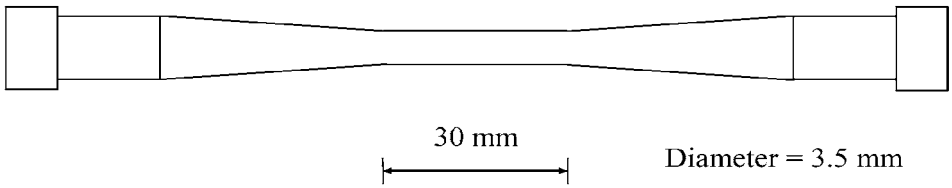

FIG. 9 ORNL Button Head Tensile Test Specimen

tensile test specimen strength data would yield a characteristic strength of $\hat{\sigma}_\theta)_a$ = 943 MPa (from Eq 13) and a mean strength of $(\bar{\sigma}_B)_a$ = 880 MPa for the flexural test specimen (from Eq 28).

9.2 *Example—Converting Characteristic Strengths: Flexure Test Specimens of Different Sizes and Loading Configurations*:

9.2.1 Table 2 shows flexural strength data from Refs **(6, 18)** for a sintered silicon carbide using both three-point and four-point configurations for sizes A, B, and C as specified in Test Method C 1161. Fractographic analyses indicated that surface-distributed flaws controlled the strengths in most specimens. Forty-eight specimens tested in the four-point B configuration confirmed that the data fit a Weibull two parameter distribution very well. Fig. 10 shows the average strengths of the specimens as a function of the effective area. The data fit the expected trend very well with the sole exception of the four-point A sized specimens. The slope of the linear-regression fitted line (area regressed on stress in this instance) is $-1/m_A$, which leads to a seventh estimate of the Weibull modulus as 14.4. The apparent deviation of the four-point A set could be simply statistical sampling error or it could be a manifestation of alignment difficulties of the small A sized specimens in a small four-point fixture.

9.2.2 This data set illustrates how data from multiple data sets can be pooled to provide superior estimates of the Weibull parameters **(6, 18)**. It is beyond the scope of this Practice at this time to specify practices for pooling data.

10. Report

10.1 Report all original test data including individual test outcomes from each test configuration that is available. Report the flaw type for each datum if possible. At the minimum, the flaw distribution type (volume, surface, edge) should be reported. Report the flaw type (e.g., inclusion, grinding crack) if possible. Report the number of test data points.

10.2 Report the original test configuration and whether the test was done in accordance with a standard. Report any deviations from procedures in the standard, if such occur.

10.3 Report the Weibull characteristic strengths, the mean strength, and the Weibull modulus for the original data set(s).

10.4 Report the Weibull material scale factor, σ_0.

10.5 Report the scaled strengths for a second (or third) test configuration.

11. Precision and Bias

11.1 Accurate and precise scaling estimates can only be obtained if the assumptions in section 5.5 are met. In particular, the flaw types must be the same in each type test configuration and the test data must be nearly error free. The stresses must be accurately known.

11.2 All Weibull parameters produced from test sets are estimates of population parameters. As such, the estimates from small numbers of test specimens (e.g., 10, 30) are subject to small sample size statistics. The Weibull modulus is especially sensitive to statistical fluctuations. Consult Practice C 1239 for guidance on statistical variations and confidence intervals for the Weibull parameter estimates. It is beyond the scope of this Practice at this time to specify confidence intervals for the scaled strength parameters.

11.3 Reference **(5)** has a compilation of many successful Weibull strength scaling exercises from a number of studies using many different test configurations.

12. Keywords

12.1 advanced ceramics; censored data; effective area; effective volume; fractography; fracture origin; size scaling; strength; Weibull characteristic strength; Weibull modulus; Weibull scale parameter; Weibull statistics

TABLE 2 Sintered Silicon Carbide Flexural Strength Data from Refs (6, 18)

Configuration	Number of Specimens Tested	Average Strength (MPa)	Std. Dev. (MPa)	m_A Weibull Modulus Estimated from the Set	σ_{oB} Weibull Material Scale Parameter Estimated from the Set	
					MPa·mm$^{2/m}$	(MPa·m$^{2/m}$)
3-point A	18	388	33	14.6	431	(167)
4-point A	17	313	35	9.4	459	(106)
3-point B	18	351	31	12.2	450	(145)
4-point B	48	303	24	14.3	430	(164)
3-point C	18	326	22	16.4	419	(180)
4-point C	18	284	22	14.5	441	(170)

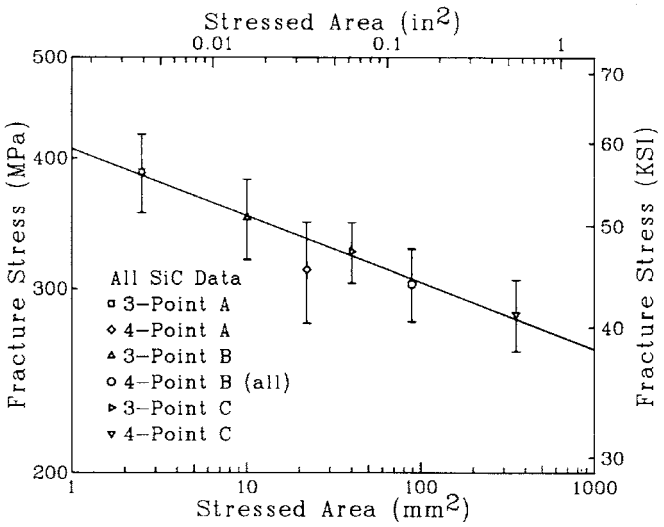

NOTE—The uncertainties are one standard deviation. Regression of the mean strengths as a function of stressed area provides another good estimate of the Weibull modulus.

FIG. 10 Average Flexural Strengths of Sintered Silicon Carbide as a Function of Weibull Effective Area for All Six Testing Configurations in Test Method C 1161

ANNEXES

(Mandatory Information)

A1. COMBINED GAMMA FUNCTION FOR ROUND RODS TESTED IN FLEXURE

A1.1 The effective volume and effective surface expressions for rod tested in flexure includes a term that combines several Gamma functions:

$$G = \left(\frac{\Gamma\left(\frac{m_V + 1}{2}\right)\Gamma\left(\frac{3}{2}\right)}{\Gamma\left(\frac{m_V + 4}{2}\right)} \right) \quad \text{(A1.1)}$$

A1.1.1 G only depends upon the Weibull modulus. Fig. A1.1 shows how G varies with m. Use m_V for volume-distributed flaws, or m_A for surface-distributed flaws.

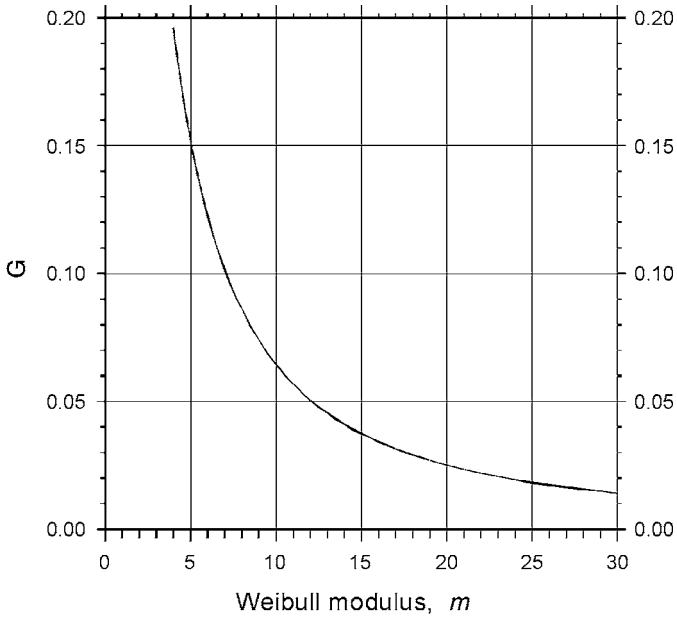

FIG. A1.1 *G*, the Combined Gamma Function is a Function of the Weibull Modulus

A2. COMPONENTS OR TEST SPECIMENS WITH MULTIAXIAL STRESS DISTRIBUTIONS

A2.1 Many test configurations have multiaxial tensile stress states. Each tensile stress component may contribute to the risk of rupture.

A2.2 The Principal Independent Action (PIA) model simply assumes that each principal stress contributes independently to the risk of rupture for each volume or area sub element in a body. Other multiaxial failure criteria may be based on different mechanics principles, but there is no consensus on the best model for all cases. The best criterion probably varies with flaw type and material. The simple PIA model lends itself to the complex integrations necessary to compute the effective surfaces and volumes. The latter usually do not differ significantly whether the PIA or more complex models are used. Reference **(12)** compares the criteria for one material. However, the solutions are sensitive to Weibull modulus.

A2.3 For volume-distributed flaws, the effective volume is:

$$V_e = kV = \int_V \left(\frac{\sigma_1}{\sigma_{max}}\right)^m + \left(\frac{\sigma_2}{\sigma_{max}}\right)^m + \left(\frac{\sigma_3}{\sigma_{max}}\right)^m dV \qquad \text{(A2.1)}$$

where σ_{max} is the maximum stress, and σ_1, σ_2, and σ_3 are the principal stresses (tensile) in each element of the test specimen or component.

A2.4 For surface-distributed flaws, the effective area is:

$$S_e = kA = \int_A \left(\frac{\sigma_1}{\sigma_{max}}\right)^m + \left(\frac{\sigma_2}{\sigma_{max}}\right)^m dA \qquad \text{(A2.2)}$$

where σ_{max} is the maximum stress, and σ_1 and σ_2 are the principal stresses (tensile) in each element of the test specimen or component.

A2.5 If closed form stress solutions are not available for a test specimen or component, then Eq A2.1 and A2.2 can be determined numerically, element-by-element, from finite element analysis as described in Annex A3.

A3. COMPONENTS OR TEST SPECIMENS WITH COMPLEX GEOMETRIES AND STRESS DISTRIBUTIONS

A3.1 *Effective Volume and Area Relationships for Components with Complex Stress States*:

A3.1.1 As indicated in section 6.3, expressions for $V_E(kV)$ can be obtained by setting Eq 1 equal to Eq 3, after the integration of Eq 3 has been performed over the gage section of the test specimen. Expressions for $S_E(kA)$ also can be obtained by setting Eq 1 equal to Eq 9, after the integration of Eq 9 has been performed over the gage section of the test specimen. This approach requires the values of m, σ_θ, and a closed form integration of Eq 3 or Eq 9. For many test specimen geometries Eq 3 or Eq 9 cannot be integrated to yield a closed form solution. A numerical integration of Eq 3 or Eq 9 can be performed using structural reliability algorithms such as *CARES* **(19)**, *ERICA* **(20)**, *STAU* **(21)**, *CERAM* **(22)**, or

GFICES (**23**) and the results can be utilized to compute either *kV* or *kA* for a specific test specimen geometry. The procedure for obtaining results using this numerical approach are outlined in this appendix.

A3.1.2 For a test specimen geometry fabricated from a given ceramic, the failure data for volume-distributed flaws is analyzed and m_V as well as $(\sigma_\theta)_V$ are obtained using maximum likelihood estimators. Note that $(\sigma_\theta)_V$ is not relevant to the computation of V_E, but is required for the computation of $(\sigma_0)_V$ utilizing the approach outlined in this section. A finite element analysis of the test specimen geometry is conducted using a sufficiently refined mesh. In the process of refining a mesh for a given test specimen geometry an asymptotic value of V_E is used to assess when a quality mesh has been attained. As an example consider a C-ring test specimen geometry discussed in section 7.4. Duffy et al. (**24**) conducted analytical studies and published figures similar to Fig. A3.1 in the process of verifying the expressions listed in section 7.4. Note the asymptotic behavior as the density of the mesh increases.

A3.1.2.1 In order to generate a relationship between V_E and the finite element mesh, utilize Eq 3 but with:

$$(\sigma_0)_V = (\sigma^*)_V \tag{A3.1}$$

where σ* is an arbitrary, assumed estimate of the Weibull material scale factor. This yields:

$$P_f = 1 - \exp\left[\int_V \left(\frac{\sigma}{(\sigma^*)_V}\right)^{m_V} dV\right] \tag{A3.2}$$

A3.1.2.2 Rearranging Eq A3.2 yields:

$$P_f = 1 - \exp\left[-\left(\frac{\sigma_{MAX}}{(\sigma^*)_V}\right)^{m_V} \int_V \left(\frac{\sigma}{\sigma_{MAX}}\right)^{m_V} dV\right] \tag{A3.3}$$

where σ_{MAX} is an equivalent (or effective) normalizing stress obtained from a *CARES* (**19**), *ERICA* (**20**), *STAU* (**21**), *CERAM* (**22**), or *GFICES* (**23**) analysis. Now define:

$$V_E = kV = \int_V \left(\frac{\sigma}{\sigma_{MAX}}\right)^{m_V} dV \tag{A3.4}$$

A3.1.2.3 Substitution into Eq A3.2 yields:

$$P_f = 1 - \exp\left[-kV\left(\frac{\sigma_{MAX}}{(\sigma^*)_V}\right)^{m_V}\right] \tag{A3.5}$$

A3.1.2.4 Solving this expression for *kV* results in:

$$kV = \frac{-\ln(1 - P_f)}{\left[\frac{\sigma_{MAX}}{(\sigma^*)_V}\right]^{m_V}} \tag{A3.6}$$

A3.1.2.5 The finite element analysis of the test specimen geometry and the resulting component probability of failure (P_f) must be computed using m_V obtained from the maximum likelihood estimators in accordance with Practice C 1239. The resulting component probability of failure (P_f) is inserted into Eq A3.5 along with the assumed value of $(\sigma_0)_V$ (= σ*), m_V, and σ_{MAX}. The effective volume of the test specimen geometry is calculated directly from Eq A3.6.

A3.1.3 A similar analysis can be conducted in order to determine an effective area (S_E, *kA*) for a given test specimen geometry. Here:

$$S_E = kA = \frac{-\ln(1 - P_f)}{\left[\frac{\sigma_{MAX}}{(\sigma^*)_A}\right]^{m_A}} \tag{A3.7}$$

A3.1.4 Alternatively, the integrals:

$$S_E = kA = \int_A \left(\frac{\sigma_1}{\sigma_{MAX}}\right)^{m_A} + \left(\frac{\sigma_2}{\sigma_{MAX}}\right)^{m_A} dA \tag{A3.8}$$

and

$$V_E = kV = \int_V \left(\frac{\sigma_1}{\sigma_{MAX}}\right)^{m_V} + \left(\frac{\sigma_2}{\sigma_{MAX}}\right)^{m_V} + \left(\frac{\sigma_3}{\sigma_{MAX}}\right)^{m_V} dV \tag{A3.9}$$

can be determined numerically element-by-element from the finite element analysis output where σ_{MAX} is the maximum tensile stress in the model and σ_1, σ_2 and σ_3 are the principal stresses (tensile) at the integration points in any element:

$$S_E = kA = \sum_{i=1}^{n} \left[\left(\frac{\sigma_{1i}}{\sigma_{MAX}}\right)^{mA} + \left(\frac{\sigma_{2i}}{\sigma_{MAX}}\right)^{m_A}\right] \tag{A3.10}$$

$$V_E = kV = \sum_{i=1}^{n} \left[\left(\frac{\sigma_{1i}}{\sigma_{MAX}}\right)^{mV} + \left(\frac{\sigma_{2i}}{\sigma_{MAX}}\right)^{m_V} + \left(\frac{\sigma_{3i}}{\sigma_{MAX}}\right)^{m_V}\right] \tag{A3.11}$$

where *n* is the number of elements with tensile (positive) stresses (**25**).

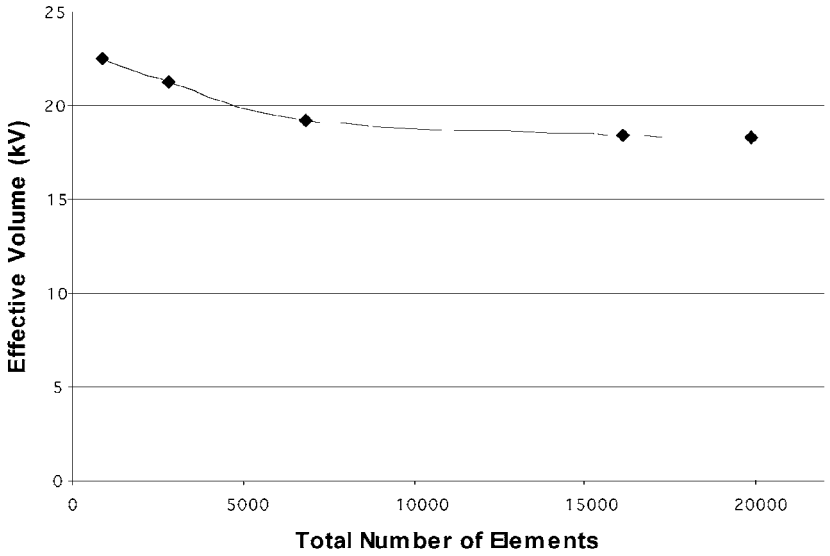

FIG. A3.1 Asymptotic Behavior of $V_E(kV)$ as a Function of Mesh Size for a C-Ring Test Specimen

REFERENCES

(1) Mann, N. R., Schafer, R. E., and Singpurwalla, N. D., *Methods for Statistical Analysis of Reliability and Life Data*, John Wiley & Sons, New York, NY, 1974.

(2) Kalbfleisch, J. D., and Prentice, R. L., *The Statistical Analysis of Failure Time Data*, John Wiley & Sons, New York, NY, 1980.

(3) Lawless, J. F., *Statistical Models and Methods for Lifetime Data*, John Wiley & Sons, New York, NY, 1982.

(4) Nelson, W., *Applied Life Data Analysis*, John Wiley & Sons, New York, NY, 1982.

(5) Quinn, G. D., and Morrell, R., "Design Data for Engineering Ceramics: A Review of the Flexure Test," *Journal of the American Ceramic Society*, Vol 74, No. 9, Sept. 1991, pp. 2037–2066.

(6) Johnson, C. A., and Tucker, W. T., "Advanced Statistical Concepts of Fracture in Brittle Materials," *Ceramics and Glasses, Engineered Materials Handbook*, Vol 4: S. J. Schneider, tech. chair., 1991, pp. 709–715.

(7) Jayatilaka, A de S., *Fracture of Engineering Brittle Materials*, Applied Science Publ., London, 1979.

(8) Weil, N. A., and Daniel, I. M., "Analysis of Fracture Probabilities in Nonuniformly Stressed Brittle Materials," *Journal of the American Ceramic Society*, Vol 47, No. 6, June 1964, pp. 268–274.

(9) Quinn, G. D., "Weibull Strength Scaling for Standardized Rectangular Flexure Specimens," *Journal of the American Ceramic Society*, Vol 86, No. 3, March 2003, pp. 508–510.

(10) Quinn, G. D., "Weibull Effective Volumes and Surfaces for Cylindrical Rods Loaded in Flexure," *Journal of the American Ceramic Society*, Vol 86, No. 3, March 2003, 475–479.

(11) Jadaan, O. M, Shelleman, D. L., Conway, Jr., J. C., Mecholsky, Jr., J. J., and Tressler, R. E., "Prediction of the Strength of Ceramic Tubular Components: Part 1–Analysis," *Journal of Testing and Evaluation*, Vol 19, No. 3, March 1991, pp. 181–191.

(12) Salem, J. A., and Adams, M., "The Multiaxial Strength of Tungsten Carbide," *Ceramic Engineering and Science Proceedings*, Vol 20, No. 4, 1999, pp. 459–466.

(13) Barnett, R. L., Connors, C. L., Hermann, P. C., and Wingfield, J. R., "Fracture of Brittle Materials Under Transient Mechanical and Thermal Loading," U. S. Air Force Flight Dynamics Laboratory, AFFDL-TR-66-220, March 1967.

(14) Salem, J. A. and Power, L., "Guidelines for the Testing of Plates," *Ceramic Engineering and Science Proceedings*, 24 [3-4], 2003, pp. 351–364.

(15) Andrews, M. J., Wereszczak, A. A, Kirkland, T. P., and Breder, K., "Strength and Fatigue of NT551 Silicon Nitride and NT551 Exhaust Valves," ORNL TM-1999/332, U.S. Department of Energy, 1999.

(16) Johnson, C. A., "Fracture Statistics of Multiple Flaw Populations," *Fracture Mechanics of Ceramics*, Vol 5, R. C. Bradt, et al, eds., 1983, pp. 365–386.

(17) Jenkins, M. G., Ferber, M. K., Martin, R. L., Jenkins, V. T., and Tennery, V. J., "Study and Analysis of the Stress State in a Ceramic, Button-Head, Tensile Specimen," ORNL TM-11767, Oak Ridge National Laboratory, 1991.

(18) Johnson, C. A. and Tucker, W. T., "Weibull Estimators for Pooled Fracture Data," *Life Prediction Methodologies and Data for Ceramic Materials*, ASTM STP 1201, eds. C. R. Brinkman and S. F. Duffy, ASTM, Philadelphia, PA 1994, pp. 250–264.

(19) Nemeth, N. N., Powers, L. M., Janosik, L. A., and Gyekenyesi, J. P., *Ceramics Analysis and Reliability Evaluation of Structures Life Prediction Program (CARES/LIFE) Users and Programmers Manual*, 1993.

(20) Schenk, B., Brehm, P. G., Menon, M. N., Tucker, W. T., and Peralta, A. D., "Status of the CERAMIC/ERICA Probabilistic Life Prediction Codes Development for Structural Ceramic Applications," ASME paper 99-GT-318, presented at the International Gas Turbine and Aeroengine Congress and Exposition, Indianapolis, IN, USA, June 7–10, 1999.

(21) Heger, A., Brückner-Foit, A., and Munz, D., "STAU—A Computer Code to Calculate the Failure Probability of Multiaxially Loaded Ceramic Components," *Euroceramics II, Vol 2, Structural Ceramics and Composites*, eds. G. Ziegler and H. Hausner, German Ceramic Society, Berlin, 1991, pp. 1143–1147.

(22) Lamon, J., "Reliability Analysis of Ceramics Using the CERAM Computer Program," ASME paper 90-GT-98, presented at the Gas Turbine and Aeroengine Congress and Exposition, Brussels, Belgium, June 11–14, 1990.

(23) Suzuki, A. and Hamanaka, J., "Design Guide for Fine Ceramics Components," *IHI Engineering Review*, 26[4], 1993, pp. 133–137.

(24) Duffy, S. F., Baker, E. H., Wereszczak, A. A., and Swab, J. J.,

"Weibull Analysis Effective Volume and Effective Area for a Ceramic C-Ring Test Specimen," *ASTM Journal of Testing and Evaluation*, Vol 33, No. 4, July 2005, pp. 233–238.

(**25**) Powers, L. M., Starlinger, A., and Gyekenyesi, J. P. "Ceramic Component Reliability with the Restructured NASA/Cares Computer Program," NASA TM-105856, National Aeronautics and Space Administration, 1992.